General imaging of advanced 3D mask objects based on the fully-vectorial Extended Nijboer-Zernike (ENZ) theory

Sven van Haver*[a], Olaf T.A. Janssen[a], Joseph J.M. Braat[a], Augustus J.E.M. Janssen[b], H. Paul Urbach[a] and Silvania F. Pereira[a]

[a]IST-Optics Research Groep, Delft University of Technology, Lorentzweg 1, NL-2628 CJ Delft, The Netherlands;
[b]Philips Research Europe, HTC 36, NL-5656 AE Eindhoven, The Netherlands

ABSTRACT

In this paper we introduce a new mask imaging algorithm that is based on the source point integration method (or Abbe method). The method presented here distinguishes itself from existing methods by exploiting the through-focus imaging feature of the Extended Nijboer-Zernike (ENZ) theory of diffraction. An introduction to ENZ-theory and its application in general imaging is provided after which we describe the mask imaging scheme that can be derived from it. The remainder of the paper is devoted to illustrating the advantages of the new method over existing methods (Hopkins-based). To this extent several simulation results are included that illustrate advantages arising from: the accurate incorporation of isolated structures, the rigorous treatment of the object (mask topography) and the fully vectorial through-focus image formation of the ENZ-based algorithm.

Keywords: Mask imaging, Extended Nijboer-Zernike (ENZ), mask topography effects, Abbe method, vectorial, non-periodic objects, FDTD

1. INTRODUCTION

Mask technology has always been essential in optical lithography and is expected to be even more critical for future nodes. Driven by Moore's law, the amount of information placed on a mask grows exponentially and this trend is only intensified by the introduction of reticle enhancement techniques such as optical proximity correction (OPC).[1] Consequently, reticles can no longer be considered as simple binary representations of the desired wafer pattern and have evolved to very complex structures that shape both the amplitude and phase of the transmitted or, for EUV, reflected light. Contemporary reticles contain features that are of the same order of magnitude as the wavelength and often show more resemblance with diffractive optical elements than with the wafer pattern they tend to produce.

As an essential part of the lithographic process, mask technology is under constant pressure to perform better. The complexity and information density of the reticle has been increasing with every node in the lithographic roadmap, while at the same time error margins have become more and more narrow. This poses a great challenge for the mask making community, not only in terms of manufacturability, but also for the mask design process itself. Nowadays, this process consists of an iterative procedure because the complex relation between the reticle and desired wafer pattern does not allow for a direct design approach.

An important aspect of the mask design process is the ability to predict the resulting image for a given mask object in an accurate and reliable manner. The vast majority of mask imaging algorithms used by the mask making community today, are based on Transmission Cross-Coefficients (TCC) computations,[2] using the so-called Hopkins approximation.[3] Although this approach can be very computationally efficient it is based on certain approximations and assumptions that do not necessarily hold for the complex mask geometries encountered in the present and future nodes of the lithographic roadmap. The problems related to the applicability of the TCC-method have been recognized for quite some years now, and have attracted a large interest by the lithographic community. In this paper we present an alternative to the established algorithms that in principle can deal with these complex mask objects in a more accurate manner.

*s.vanhaver@tudelft.nl, Tel: +31 (0)15 2782116, Fax: +31 (0)15 2788105, Url: http://www.nijboerzernike.nl

In Section 2 of this paper we will briefly introduce the Extended Nijboer-Zernike (ENZ) theory of diffraction and describe the mask imaging algorithm that can be constructed from it. In Section 3 we will identify and discuss some of the specific areas in which the ENZ-based mask imaging algorithm is beneficial compared to those based on the Hopkins approach. Subsequently, some examples are included in Section 4 to illustrate our findings and we will end this paper with some concluding remarks in Section 5.

2. METHODOLOGY

The imaging algorithm we present here can be categorized as a source point integration method (also called Abbe's method). The difference with existing algorithms based on this method lies in the fact that our algorithm applies a pupil diffraction routine that is based on the Extended Nijboer-Zernike theory of diffraction. Below we give a short introduction into the ENZ-theory followed by a description of the mask imaging scheme that can be constructed from it.

2.1 The Extended Nijboer-Zernike theory of diffraction

The ENZ-theory of diffraction originates from two papers[4,5] published in 2002. In these papers a semi-analytic solution to the Debye diffraction integral for the imaging of a point source by a general optical system, was introduced. The development of the ENZ-theory was intended to provide a method to characterize optical systems by means of intensity measurements in the focal region.[6] In order to achieve this, it was fundamental to have both an accurate and fast algorithm to compute the point-spread function for a general aberrated system. In terms of computations, this comes down to computing the point-spread function from the otherwise uniform exit-pupil, for an exit-pupil that is influenced by a general aberration. Although the non-uniformities, present in the pupil due to aberrations, are usually small and should be relatively small in order to make ENZ-characterization possible, the pupil diffraction method itself is not limited by the size of the deformations and can be applied to general pupils. Recognizing the fact that in mask imaging one also needs to produce an image from an exit-pupil distribution that is in general very complex, both in amplitude and phase, we believe that this appealing feature of ENZ-theory is well suited to be exploited in the field of mask imaging.

2.2 The ENZ-based mask imaging scheme

For imaging systems that satisfy, for example, the Abbe-sine condition,[7] one can construct an ENZ-based mask imaging scheme as follows:

1. As we are applying a source point integration method, we start by discretizing the illumination source. The light coming from a single source-point is collected by the illumination optics and gives rise to a plane wave incident on the mask. Here, the angle of incidence of the plane wave is determined by the spatial position of the source point under consideration.

2. A rigorous electromagnetic solver is applied to compute the near-field resulting from the interaction between the incident plane wave and the mask. For the examples found in this paper we have used an in-house developed FDTD implementation,[8] but, in principle, any rigorous solver can be used.

3. The near-field at the mask resulting from the electromagnetic computations is subsequently propagated to the entrance pupil. As the active region of the mask is very small compared to the aperture of the projection optics, it is allowed to apply the Fraunhofer approximation, where in the general case the entrance pupil is given as a spherical surface.

4. Having the field in the entrance pupil of the imaging system available, this allows us to apply the imaging algorithm provided by ENZ-theory and obtain the aerial-image contribution due to a single illumination point-source.

5. Finally, step 1-4 should be repeated for every point source present in the light source and their contributions are summed incoherently to obtain the aerial-image of the mask produced by the imaging system.

In the scheme above, steps 1-3 are common to all source point integration methods. This method is not widely used by the mask making community because it is far less computationally efficient compared with methods based on the Hopkins approach.[2] Nevertheless, the scheme given above enables a large gain in computational efficiency that stems from a highly structured use of basic functions in the ENZ imaging routine. Although speed is critical in mask simulation, it is not this feature of the ENZ scheme that is most important. The fact that this method does not presume periodicity in the object and allows a full vectorial treatment (a vectorial version of ENZ-theory is available for the mask imaging process[9,10,11]), will result in greater accuracy as compared to the established algorithms. A more extensive discussion on this is presented in the next section.

3. HOPKINS VERSUS ENZ

The method presented in this paper has some fundamental differences compared to the established methods that are based on the Hopkins approach.[3] First of all, our method deals with isolated structures instead of infinitely repeated objects that are required by most other methods. As an infinitely periodic object is merely a mathematical construction that enhances computational efficiency, it of course has no physical relevance in the lithographic process itself. As a matter of fact, the established methods require significant 'zero padding' around the mask-region of interest in order to obtain accurate simulation results for the image of an isolated structure. Based on these observations it seems only natural to favor a method that presumes a realistic isolated object in order to obtain the highest possible simulation accuracy.

In addition, many algorithms commonly used by the mask making community still apply the thin mask approximation. In this approximation, one assumes that the field transmitted by the mask changes abruptly according to the transmittance of the mask. Although physically incorrect, this approach has proved to be sufficient in the past for most lithographic simulations. Nevertheless, the feature sizes and relative mask thickness encountered in simulations today, do no longer allow for the thin mask approximation to be applied. As a result, the Hopkins approximation, which states that the diffraction orders of a mask that is illuminated under an oblique angle can be obtained by a simple shift of the spectra of the mask under normal incidence, also no longer holds. Instead, for every illumination angle a rigorous electromagnetic solver should be used to accurately describe the interaction between the incident illumination and the mask, after which the resulting complex vector field at the mask should serve as the input for the remainder of the computation scheme. This is exactly the approach taken in the scheme presented in Section 2.2.

The third advantage of our method is the fact that it can straightforwardly be extended to operate fully vectorially. As already mentioned in the previous section, a fully vectorial version of the ENZ-formalism is available. This means that, for a given complex vector field in the entrance pupil, one can compute both the electric and magnetic vector fields in the image region of the imaging system. Note that in the computation of these quantities the radiometric effect[12] and possible aberrations (both amplitude and phase) are included in the ENZ-theory. Especially for the hyper-NA systems encountered in immersion lithography, a vectorial treatment of the imaging process is indispensable. For the Hopkins based methods, several attempts have been undertaken to expand them vectorially, but none of them have been totally satisfactory.

One might argue that the points discussed above are of little importance. After all, methods based on the Hopkins approach have proven to be applicable to lithographic simulations in several decades of succesful operation. However, the ongoing drive for further miniaturization of electronic circuits has resulted in mask designs that currently contain features with a size equal or smaller then the wavelenght of the light used in the lithographic process.[1] Despite the fact that the contributions discussed above are small, they are significant in this regime and tend to get even more important in future lithographic practice. Based on these observations we believe that the method presented here can be a valuable contribution to existing algorithms as it provides a more physical computation approach which in principle is far more accurate.

4. SIMULATIONS

In this section we present some mask simulations performed with the calculation scheme as introduced in Section 2.2. The examples presented here aim on illustrating some of the advantages of the ENZ-based scheme over more conventional methods.

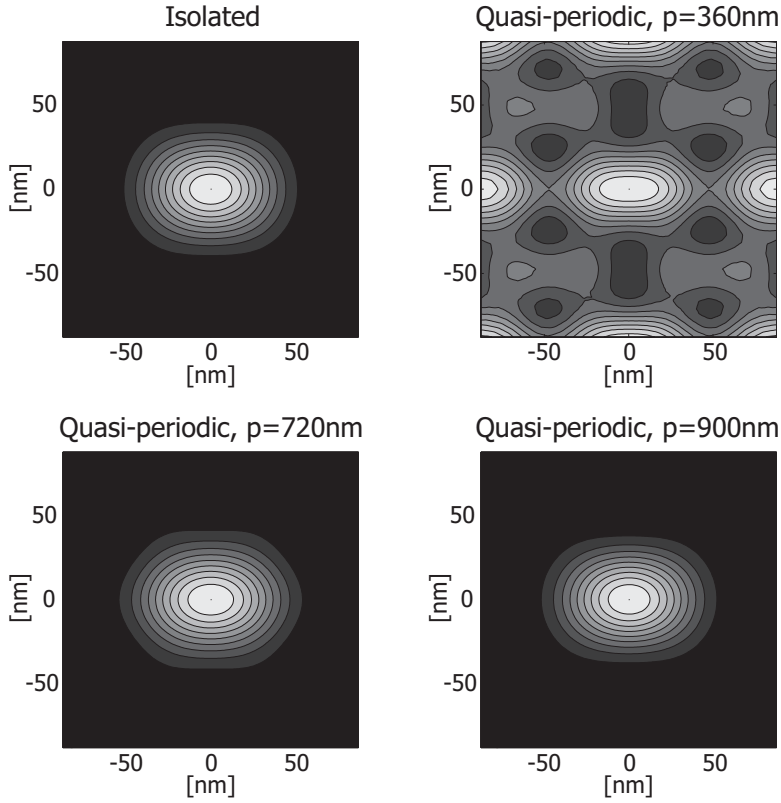

Figure 1. This figure illustrates the difference between periodic and non-periodic mask imaging. A period $p = 360$nm is clearly unsufficient to image the 180nm contact hole. Doubling the period to $p = 720$nm helps (RMS $\approx 2\%$), but a period as large as $p = 900$nm is required to obtain an accurate (RMS $< 1\%$) quasi-isolated image (imaged by a lithographic immersion system; $\lambda = 193$nm, NA $= 2.2$, reduction 4x).

4.1 Periodic versus non-periodic computations

As already discussed above, one of the most apparent differences between conventional and ENZ-based methods is the fact that one is periodic and the other is non-periodic. Now, since many mask simulations investigate the printability of a certain specific mask structure, this means that one mostly deals with an isolated non-periodic mask object. The way in which such structures are dealt with in the periodic methods involves a large increase of the period by means of zero-padding around the region of interest. Of course a large period is undesired as it will increase the computational burden. In Fig.1 we illustrate the effects introduced by a periodic treatment of the object. We have computed the image produced by a mask with a 180nm contact hole that is illuminated by 193nm x-polarized light at normal incidence. The top-left figure shows the resulting image for the isolated structure (imaged by a lithographic immersion system; NA $= 2.2$, reduction 4x) computed with the non-periodic ENZ-algorithm. The top-right picture shows a simulation of the same contact hole, except that the object is quasi-periodic with a unit cell of 360x360nm. (Note that we speak of quasi-periodicity as we consider a mask with a 3x3 formation of the unit cell, instead of a real periodic object which can not be treated directly by our simulation tool.) It is clear from this image that the period should be increased to obtain an accurate prediction for the image for a single hole. In the bottom-left picture the exercise has been repeated for the same contact hole, but now with a doubled period (unit cell is 720x720nm). Finally, the bottom-right picture shows the image for a unit cell of 900x900nm. Although, the bottom-left image is far better than the top-right image, there are still distinct differences with the isolated case (top-left image). One should consider a unit cell as large as 900x900nm to closely resemble the isolated case. This effectively means that for an equally accurate periodic treatment of this contact hole, we have to consider a computational domein that is at least 4 times larger

than what it should be for an ENZ-based computation. This exercise has shown that the ENZ-based algorithm requires a far smaller mask area to be considered in order to obtain accurate images of isolated structures and that if a periodic methods is used, great care should be taken in defining a large enough unit cell in order to achieve realistic results.

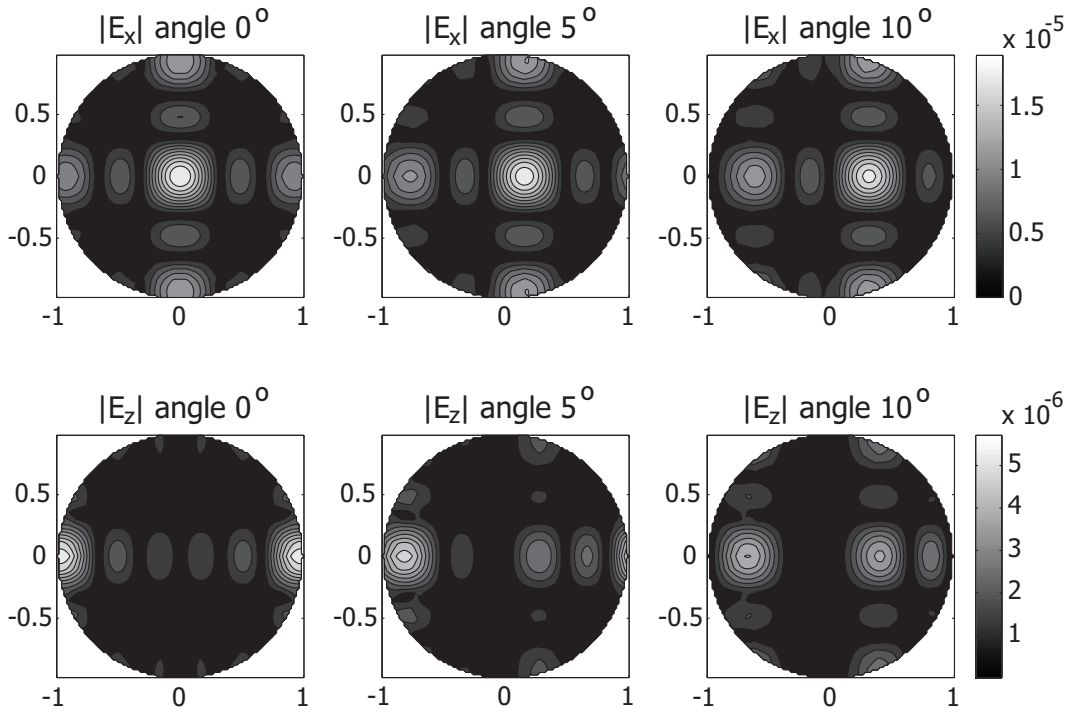

Figure 2. This figure illustrates the breakdown of the Hopkins approximation induced by topography effects. The top and bottom row of pictures represent the $|E_x|$ and $|E_z|$ components of the electric field in the spherical entrance pupil, projected onto the xy-plane. (Note that we have used normalized pupil coordinates.) Especially in the z-component one can observe that the field obtained at an oblique angle can not simply be represented by a shifted version of the normal incidence field (angle $= 0^o$).

4.2 Mask topography effects

The second and third difference discussed in Section 3 are both closely related to possible issues arising from the complex mask topography presently encountered in mask technology. The sub-wavelength features on the mask place a serious limitation on the Kirchhoff boundary conditions, that replace the field on the mask openings by the incident field, since this approximation fails to account for the increasingly important topographical effects (thick mask effects) in the computation of the lithographic image. Closely related to the limitations of the Kirchhoff boundary conditions is the applicability of the Hopkins approach, as it is based on this approximation. As a result the Hopkins approximation is also violated when masks with a complex topography are considered.[13] In Fig. 2 we illustrate the breakdown of the Hopkins approximation. In this figure we show the $|E_x|$ and $|E_z|$ field components in the entrance pupil, produced by a 3x3 array of 180nm contact holes mask object. The columns is this figure pertain to three different illumination states incident on the mask, all of them x-polarized but with different incidence angles of 0, 5 and 10 degrees in the x-direction. Whereas the Hopkins approach predicts that the field in the entrance pupil should be equal for all incidence angles apart from a lateral shift, this is clearly not the case in this example. Especially the z-component shows a distinct non-lineair dependence on the incidence angle.

The limitations of the Hopkins approach, as illustrated in Fig 2, are well known and have caused a large concern by the lithographic community in recent years[14,15,16]. In fact, extensions have been developed to accomodate for these mask topography effects[17,18]. Although, the most appropriate way to deal with this issue would be to replace the Kirchhoff boundary conditions approach by a rigorous treatment of the electromagnetic boundary problem, there remains a large threshold in applying this approach due to the large computational implications. As a result, many alternative model-based methods have been proposed that try to include the main topography effects[19,20]. Although these methods have proven to be sufficient for the time being, we see them merely as temporary solutions as the ongoing shrinkage of mask features demands for more and more topography effects to be included. For this reason we have chosen to adhere to the full rigorous treatment in the ENZ mask imaging algorithm.

Simply treating the mask rigourously is not enough to incoporate mask topography effects completely. One should also be able to accurately image the vector field resulting from the rigourous computation. Over the years, extensions to the TCC method have been developed that perform imaging of the exit pupil in a fully vectorial manner, making it possible to do so-called resist imaging.[21] Although lithographic simulations based on this extended TCC approach are generally considered to be fully vectorial this is not necessarily the case. In the original paper by Flagello et al.[22], the z-component of the electric field transmitted by the mask is neglected. At the time this simplified treatment was allowed as the object side numerical-aperture remained relatively small ($\mathrm{NA}_{obj} < 0.2$). Nevertheless, in contemporary lithographic systems the object side numerical-aperture can be considerably larger. Combined with the fact that lithographic printing has become very critical, making even the smallest contributions significant, it has become important to include even the small contribution introduced by the z-component of the electric field originating from the mask. In the ENZ-based mask imaging algorithm this z-component is correctly included, allowing the statement that this algorithm is truly a fully vectorial mask imaging method.

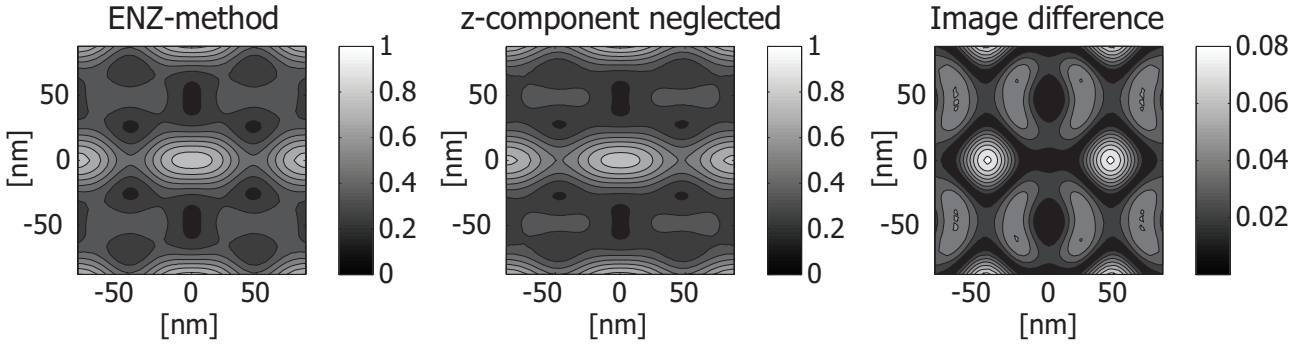

Figure 3. This figure illustrates the error due to discarding the z-component of the field originating from the mask.

In the final example presented in this section, we illustrate the influence of correctly including the z-component of the electric field. For the simulation of the images shown in Fig. 3 we have again taken the object to be a 3x3 array of 180nm contact holes. The aerial image of this mask object, when illuminated by x-polarized light under normal incidence, is computed for imaging by an immersion lithographic system ($\lambda = 193$nm, NA = 2.2 and reduction 4x). In the left-most figure the image computed with the ENZ-algorithm is shown. For the computation of the image in the middle figure the same algorithm was used, only this time the z-component of the electric field emerging from the mask was neglected. The error induced by this simplification is displayed in the third figure. For this merely academic example, with a numerical aperture value that most propably will never be reached, the error introduced by neglecting the z-component is as large as 8 percent of the maximum peak intensity in the image, but also for systems with a more realistic numerical aperture value, say NA = 1.44, the corresponding error will still exceed a few percent. In advanced lithography, contributions of this magnitude are certainly significant and therefore one should include the z-component during simulations. Note that the ENZ-based algorithm does not pay an additional computational penalty upon including this component.

5. CONCLUSIONS

In this paper we have presented a new mask imaging algorithm that can be categorized as a source-point integration (Abbe) method. Compared to the more conventional transmission cross-coefficient (Hopkins) based methods, the Abbe method relies on less approximations and is therefore expected to be more accurate. Unfortunately, this enhanced accuracy comes at the cost of a far larger computational burden and this is the main reason why the Hopkins based methods have dominated the mask simulation community for the past decades. The ENZ-based algorithm presented in this paper, although a variant of the Abbe method, does allow for a significant reduction of the computational burden. This reduction originates from ENZ-theory, where the structured use of basic functions can be exploited to do many computations in advance and store the results in look-up tables. Although, this reduction still does not allow the ENZ-method to compete on speed with the Hopkins method, it does enable the execution of accurate Abbe-based simulations within an acceptable time-scale.

The most attractive feature of the ENZ-based method remains its accuracy. Especially, for advanced lithographic systems that intend to image masks with a high topography, the ENZ-method is clearly more accurate than the standard Hopkins approach. Compared to the more advanced implementations of the TCC-method the differences are less pronounced but, nonetheless, some of the advantages of the ENZ-method remain. For example, to accurately include mask topography effects, advanced TCC-methods also rely on a rigorous treatment of the mask. But as the TCC-method assumes a periodic object, it was shown that it requires a far larger computational domain (or unit cell) than the ENZ-method which operates on isolated objects. This clearly results in a reduction of computational burden and hardware requirements.

The most important feature of the ENZ-algorithm is its fully vectorial treatment of the through-focus image formation. The vector field resulting from the rigorous treatment of the mask serves as the input of the ENZ-imaging algorithm without any simplifications. This in contrast to most advanced TCC-methods that discard the z-component of the electric field transmitted/refracted by the mask. As was shown in Sec. 4, this can have a significant effect on the obtained image. In the ENZ-algorithm the z-components is naturally included, without any implications on the computational efficiency.

Altogether, we believe that the ENZ-method discussed in this paper is a valuable addition to the mask imaging algorithms available to the lithographic community. Unlike conventional methods, the ENZ-method is not based on the Hopkins approach. Therefore it provides an independent alternative that, combined with its high accuracy, is especially attractive for benchmarking purposes, which is included in our plans for the coming year. In addition, by exploiting ENZ-theory it was possible to mostly remove the computational implications of the original Abbe approach. So far, this did not allow the ENZ-method to compete with any commercial mask design solution on speed. Nonetheless, the ENZ-algorithm is still in its early stages of development and does show potential te be further developed into a mask imaging solution that can face the competition in the future.

REFERENCES

1. A. K. Wong, *Resolution enhancement techniques in optical lithography*, Bellingham: SPIE Press, 2001, Tutorial texts in optical engineering Vol. TT47, 2001.
2. A. K. Wong, *Optical imaging in projection microlithography*, Bellingham: SPIE Press, 2005, Tutorial texts in optical engineering Vol. TT66, 2005.
3. H. H. Hopkins, "On the Diffraction Theory of Optical Images," *Proc. Roy. Soc. A* **217**, pp. 408–432, May 1953.
4. A. J. E. M. Janssen, "Extended Nijboer-Zernike approach for the computation of optical point-spread functions," *J. Opt. Soc. Am. A* **19**, pp. 849–857, May 2002.
5. J. J. M. Braat, P. Dirksen, and A. J. E. M. Janssen, "Assessment of an extended Nijboer-Zernike approach for the computation of optical point-spread functions," *J. Opt. Soc. Am. A* **19**, pp. 858–870, May 2002.
6. P. Dirksen, J. J. M. Braat, A. J. E. M. Janssen, A. Leeuwestein, T. Matsuyama, and T. Noda, "Aerial image based lens metrology for wafer steppers," in *Proceedings of the SPIE, Vol.*, **6154**, pp. 331–341, Apr. 2006.
7. M. Born and E. Wolf, *Principles of optics. Electromagnetic theory of propagation, interference and diffraction of light*, Oxford: Pergamon Press, 1980, 6th corrected ed., 1980.

8. O. T. A. Janssen, S. van Haver, A. J. E. M. Janssen, J. J. M. Braat, H. P. Urbach, and S. F. Pereira, "Extended Nijboer-Zernike (ENZ) based mask imaging: Efficient coupling of electromagnetic field solvers and the ENZ imaging algorithm," in *Proceedings of the SPIE, Vol.*, **6924**, Feb. 2008.
9. J. J. M. Braat, P. Dirksen, A. J. E. M. Janssen, and A. S. van de Nes, "Extended Nijboer-Zernike representation of the vector field in the focal region of an aberrated high-aperture optical system," *J. Opt. Soc. Am. A* **20**, pp. 2281–2292, Dec. 2003.
10. J. J. M. Braat, P. Dirksen, A. J. E. M. Janssen, S. van Haver, and A. S. van de Nes, "Extended Nijboer-Zernike approach to aberration and birefringence retrieval in a high-numerical-aperture optical system," *J. Opt. Soc. Am. A* **22**, pp. 2635–2650, Dec. 2005.
11. S. van Haver, J. J. M. Braat, P. Dirksen, and A. J. E. M. Janssen, "High-NA aberration retrieval with the extended Nijboer-Zernike vector diffraction theory," *Journal of the European Optical Society - Rapid publications, vol. 1 06004* **1**, June 2006.
12. B. Richards and E. Wolf, "Electromagnetic Diffraction in Optical Systems. II. Structure of the Image Field in an Aplanatic System," *Proc. Roy. Soc. A* **253**, pp. 358–379, Dec. 1959.
13. A. Erdmann, G. Citarella, P. Evanschitzky, H. Schermer, V. Philipsen, and P. De Bisschop, "Validity of the Hopkins approximation in simulations of hyper-NA (NA$>$ 1) line-space structures for an attenuated PSM mask," in *Proceedings of the SPIE, Vol.*, **6154**, pp. 167–178, Apr. 2006.
14. A. Erdmann, P. Evanschitzky, and P. De Bisschop, "Mask and wafer topography effects in immersion lithography," in *Proceedings of the SPIE, Vol.*, **5754**, pp. 383–394, May 2005.
15. M. D. Smith, T. Graves, J. D. Byers, and C. A. Mack, "The impact of mask topography on binary reticles at the 65nm node," in *Proceedings of the SPIE, Vol.*, **5754**, pp. 527–536, May 2005.
16. J. Ruoff, J. T. Neumann, E. Schmitt-Weaver, E. van Setten, N. le Masson, C. Progler, and B. Geh, "Polarization-induced astigmatism caused by topographic masks," in *Proceedings of the SPIE, Vol.*, **6730**, Oct. 2007.
17. J. Tirapu-Azpiroz and E. Yablonovitch, "Incorporating mask topography edge diffraction in photolithography simulations," *J. Opt. Soc. Am. A* **23**, pp. 821–828, Apr. 2006.
18. Y. Inazuki, N. Toyama, T. Adachi, T. Nagai, T. Suto, Y. Morikawa, H. Mohri, and N. Hayashi, "Analysis of diffraction orders including mask topography effects for OPC optimization," in *Proceedings of the SPIE, Vol.*, **6520**, Mar. 2007.
19. Q. Yan, Z. Deng, and J. Shiely, "Fast synthesis of topographic mask effects based on rigorous solutions," in *Proceedings of the SPIE, Vol.*, **6730**, Oct. 2007.
20. Y. Aksenov, P. Zandbergen, and M. Yoshizawa, "Compensation of high-NA mask topography effects by using object modified Kirchhoff model for 65 and 45nm nodes," in *Proceedings of the SPIE, Vol.*, **6154**, pp. 513–522, Apr. 2006.
21. M. S. Yeung, D. Lee, R. Lee, and A. R. Neureuther, "Extension of the Hopkins theory of partially coherent imaging to include thin-film interference effects," in *Proceedings of the SPIE, Vol.*, **1927**, pp. 452–463, Aug. 1993.
22. D. G. Flagello, T. Milster, and A. E. Rosenbluth, "Theory of high-NA imaging in homogeneous thin films," *J. Opt. Soc. Am. A* **13**, pp. 53–64, Jan. 1996.